Two-photon induced photoconductivity enhancement in semiconductor microcavities : a theoretical investigation.

H. Folliot*, M. Lynch, A. L. Bradley, T. Krug, L. A. Dunbar, J. Hegarty, and J. F. Donegan

Physics Department, Trinity College, Dublin 2, Ireland.

L. P. Barry

Department of Electronic Engineering, Dublin City University, Dublin 9, Ireland.

* corresponding author : herve.folliot@insa-rennes.fr

present address : Laboratoire de Physique des Solides, INSA (Institut National des Sciences Appliquées), 20 Avenue des Buttes de Coësmes, CS 14315, 35 043 Rennes Cedex, France

Abstract:

We provide a detailed theoretical investigation of two-photon absorption photoconductivity in semiconductor microcavities. We show that a high enhancement of the non-linear response (>10000) can be obtained due to the microcavity effect. We discuss in detail the design and performance (dynamic range, speed) of such a device with the help of an example of a AlGaAs/GaAs microcavity operating at 900nm. This device is promising for low intensity fast autocorrelation and demultiplexing applications.

OCIS codes: (040.5150) Photoconductivity; (190.5970) Semiconductor nonlinear optics including MQW

Keywords : Two-Photon Absorption; Photoconductivity; Microcavities

1. Introduction

In recent years, Two-Photon Absorption (TPA) in semiconductor photoconductive devices has emerged as an attractive, inexpensive and convenient way for autocorrelation measurements of picosecond, and sub-picosecond laser pulses. Since the first demonstration of autocorrelation using this technique [1], many commercially available devices in different materials have been examined. This work has resulted in high sensitivity characterization of short optical pulses using TPA based autocorrelators [2-17].

In addition to autocorrelation, recent work has demonstrated the possibility of using the instantaneous TPA nonlinearity for carrying out high speed functions such as optical demultiplexing and sampling for use in ultra-high capacity optical time division multiplexed (OTDM) systems. These studies used commercial 1.3 micron laser diodes with TPA of 1.55 micron signals [11,18], and showed that this technique is promising for developing high speed components for future Terabit/s optical systems.

However, TPA devices still require high optical input intensities in order to get a significant level of photocurrent, and to exceed the residual linear absorption. One way of increasing the TPA sensitivity is of course to use long active lengths but this is at the expense

of speed that may prevent its use in OTDM systems [5]. Another approach we propose here is to use a semiconductor microcavity where the length enhancement can be achieved artificially by the use of a Fabry-Pérot cavity.

To our knowledge no theory nor results have been presented on TPA photocurrent in microcavities. The enhancement of the TPA induced photoluminescence in aminopurine have been reported [19], but no theoretical insight was given. We present a detailed theoretical study of TPA photocurrent in semiconductor microcavities, and discuss the design and performances of a device working at 900nm.

2. TPA

Two-photon absorption is a transition that results from the addition of the energy, momentum, and angular momentum of two photons. When the transition considered is from the valence to the conduction band of a semiconductor, the energy sum must then be $> E_g$, where E_g is the semiconductor bandgap energy. For degenerate TPA, where the two photons have the same energy $h\nu$, we thus have $2h\nu > E_g$. In the following, we will only consider degenerate/quasi degenerate TPA.

TPA in bulk [20-29], and Quantum Well (QW) [30-37] semiconductors has been, experimentally and theoretically, extensively studied, but since high power and large tunability are needed, very little data is available, in comparison with Single Photon Absorption (SPA) in semiconductors. Moreover, theoretical predictions are more complicated, since TPA in direct bandgap semiconductors involves mixing between bands, so a large number of bands or non-parabolicity terms in addition to excitonic effects may be needed to accurately calculate TPA

coefficients [29]. Typically, the experimental TPA coefficients are given within an accuracy of a factor of two. This is often due to many factors such as simplifications in calculations, or difficulties in fully characterizing the pulses used in TPA experiments (duration, spatial fluctuations, and coupling efficiency) [5]. Comparison between bulk and QW structures is rather difficult [38], and the use of a bulk or a QW structure will depend on the anisotropy, speed, material quality and TPA enhancement considerations. This will be discussed in section 5.

3. TPA photocurrent

When both single photon absorption (SPA) α and TPA β coefficients are taken into account, the differential equation for the intensity propagation *I(z)* along the z axis of a semiconductor is:

$$\frac{dI(z)}{dz} = -\alpha I(z) - \beta I(z)^2 \qquad (1)$$

solving for *I(z)* gives [39] :

$$I(z) = I_0 \frac{e^{-\alpha z}}{1+(\beta I_0/\alpha)(1-e^{-\alpha z})} \qquad (2)$$

The SPA and TPA contribution in the total absorption can be derived as [39]:

$$I_{abs}^{SPA} = I_0\left(1-\frac{e^{-\alpha L}}{C}\right)\frac{\alpha L}{\alpha L + \ln C} \qquad (3)$$

$$I_{abs}^{TPA} = I_0\left(1-\frac{e^{-\alpha L}}{C}\right)\frac{\ln C}{\alpha L + \ln C} \qquad (4)$$

where:

$$C = 1 + (\beta I_0 / \alpha)(1 - e^{-\alpha L}) \qquad (5)$$

If the quantum efficiency of the photoconductivity is 100%, the photocurrent J is then given by:

$$J = \frac{eS}{h\upsilon}\left(I_{abs}^{SPA} + \frac{1}{2} I_{abs}^{TPA} \right) \qquad (6)$$

where S is the illuminated area.

Using this description, the useful non-linear two-photon response is then limited on the lower side by SPA, and on the high intensity side by the total absorption (Fig. 1.), so :

$$\frac{\alpha}{\beta} \le I \le \frac{1}{\beta L} \qquad (7)$$

This gives the dynamic range where TPA can be used for autocorrelation and demultiplexing applications.

When condition (7) is satisfied, (6) becomes:

$$J = \frac{eS}{2h\upsilon} \beta I_0^2 L \qquad (8)$$

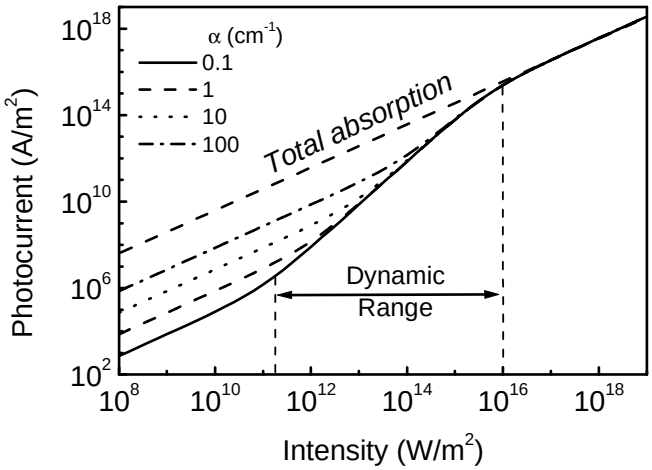

Fig. 1. Photocurrent versus intensity for a L=1μm semiconductor for different absorptions α and β=0.02 cm/MW. The dynamic range is shown for the $\alpha=0.1cm^{-1}$ curve.

Generally, in TPA photoconductivity experiments using non coherent pulses, one uses a high intensity pulse I_1 that samples a second pulse I_2. The intensity ratio between the two pulses may vary from 1:1 for autocorrelation measurements to ~1:10 for demultiplexing or sampling applications [18]. In the latter case, two non-coherent pulses produce a photocurrent proportional to $(I_1^2+2I_1I_2+I_2^2)$ so the photocurrent change (with and without the sampled pulse I_2) is proportional to $2I_1I_2$ (if I_2^2 is neglected).

For high speed demultiplexing applications, the temporal response of the device should be as fast as possible, and the TPA photocurrent should be as large as possible for low intensity optical pulses. The rise time of the photocurrent depends on the carrier collection time on both sides of the pn photodiode, whereas the fall time mainly depends on carrier diffusion to the contacts and capacitance of the diode [40]. The rise time of the TPA photocurrent can be very fast (in the order of a few ps [40], [18]), so the main limitation is due to the capacitance of the photodiode. Device capacitance can, of course, be reduced by using smaller device areas. However, in the case of optical waveguides, this implies a reduction of the TPA length and thus a reduction of TPA photocurrent, which is not desirable. A way to enhance the response time while maintaining high TPA photocurrent and low input intensity is the use of a microcavity semiconductor device.

4. TPA in microcavities

In an ideally empty tuned Fabry-Pérot cavity with front and back mirrors with amplitude reflectivities of r_1 and r_2 respectively, and a front amplitude transmission t_1, the field enhancement factor of a normal incident electric field E_0, at an antinode is given by:

$$f = \frac{t_1(1+r_2)}{(1-r_1 r_2)} \qquad (9)$$

The optical intensity is given by $I_0=E_0^2 n/2Z_0$, where Z_0 is the vacuum impedance (~377 Ω) and n is the refractive index of the medium. Thus, the intensity enhancement factor F (ratio between a cavity and non-cavity intensity), is then $F=f^2$ and, as the photocurrent depends on the square of the intensity, the enhancement factor of the photocurrent at the antinode is then F^2. For a microcavity length of λ/n, the integrated average intensity enhancement factor will be $F/2$, whereas the integrated average photocurrent enhancement factor will be $3F^2/8$. The $1/2$ and $3/8$ factors come from the average value of $I(z) \propto sin^2(k_z z)$ and $I^2(z) \propto sin^4(k_z z)$ integrated over a period $L=\lambda/n$ respectively, where k_z is the wavevector propagation on the z axis. Regarding the TPA photocurrent, the $3F^2/8$ factor can be seen as a length enhancement factor. For example, a FP cavity with a front mirror reflectivity of 0.95 and a back mirror reflectivity of 0.995 will have a length enhancement factor of around 2.5×10^4. This means that a FP cavity with a thickness of 0.3µm would have the same response as a 7.5 mm long non-cavity device, which could lead to a factor of ~10 reduction on the device surface (comparison between a 2x7500µm^2 waveguide and a 25 µm radius vertical cavity). Using a microcavity rather than a waveguide could then lead to a significant reduction of the capacitance of the device.

In fact, as the enhancement factor operates on intensity, the effective β and α coefficients now become $3F^2\beta/8$ and $F\alpha/2$ respectively.

The dynamic range, in a thick cavity, now reads:

$$\frac{4\alpha}{3F\beta} << I << \frac{8}{3F^2\beta L} \qquad (10)$$

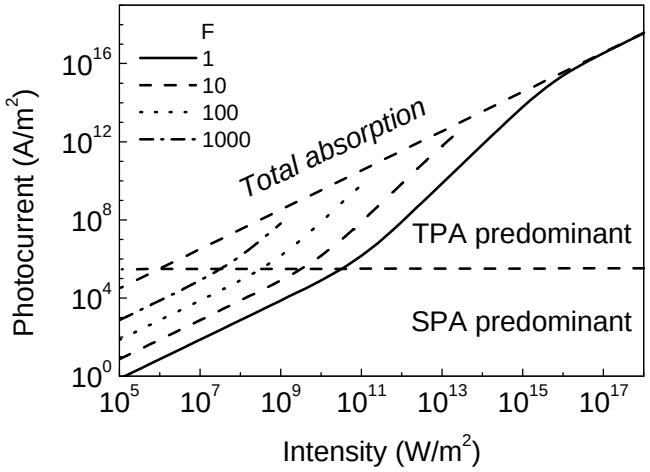

Fig. 2. Photocurrent versus intensity for a L=1μm cavity with different enhancement factors F with typical semiconductor parameters α=0.1 cm^{-1} and β=0.02 cm/MW [26]. The dashed lines show the lower (SPA predominant on TPA) and higher (total absorption) limits of the photocurrent.

Thus, the total dynamic range is given by $DR = I_{\max}/I_{\min} = 2/LF\alpha$. The microcavity response will then enhance the photocurrent but reduce the dynamic range as shown on Fig. 2.

This simple insight to microcavity enhancement does not however take into account the pulse duration or the reflectivity changes that arise from absorption and refractive index changes inside the cavity. Indeed, as TPA becomes important, the empty resonator model is no longer valid and the microcavity reflectivity tends to r_1 so the upper limit of the dynamic range has to be divided by $R_1=|r1|^2$.

To account for these changes and look at their effect on the device photoconductivity response, we have developed a simple model based on the Transfer Matrix Method (TMM).

Model :

TMM is widely used and has proven to be very effective in the description of optical properties in the linear regime. It has recently been used [41] to study TPA in Bragg reflectors. In our work, we have developed a slightly different model.

The transfer matrix method enables to write the propagation of an electric field through a multistack dielectric layer using Maxwell boundary conditions.

The transfer matrix (assuming a linear polarisation and a normal incidence angle) for the layer i relates the electric field E_i at interface i to the field E_{i+1} at interface i+1 according to :

$$\begin{bmatrix} E_i^+ \\ E_i^- \end{bmatrix} = \frac{1}{2}\begin{bmatrix} e^{ik_{i+1}d_{i+1}}\left(1+\frac{k_{i+1}}{k_i}\right) & e^{-ik_{i+1}d_{i+1}}\left(1-\frac{k_{i+1}}{k_i}\right) \\ e^{ik_{i+1}d_{i+1}}\left(1-\frac{k_{i+1}}{k_i}\right) & e^{-ik_{i+1}d_{i+1}}\left(1+\frac{k_{i+1}}{k_i}\right) \end{bmatrix}\begin{bmatrix} E_{i+1}^+ \\ E_{i+1}^- \end{bmatrix} = M_{i+1,i}\begin{bmatrix} E_{i+1}^+ \\ E_{i+1}^- \end{bmatrix} \quad (11)$$

where $k_{i,(i+1)}$ denotes the linear propagation constant in layer i (i+1) and $d_{i,(i+1)}$ the thickness of layer i (i+1) respectively. E_i^+ and E_i^- are the forward and backward propagating electric fields. It is thus possible to write the intensity profile ($I(z)=E(z)2n(z)/2Z_0$), inside a given multistack dielectric layer. In our model, for a given incoming electric field E_o^+ (and thus a given incoming intensity), we take this calculated intensity profile, to modify the propagation constant k_i which now takes into account the non-linear response of the materials. This produces a new intensity profile which generates a new set of $k_i(I(z))$ propagation constants. This procedure is then repeated until convergence is reached. The convergence criterion is choosen to be the integrand of the squared intensity profile difference along z between two

adjacent self consistent calculation steps. The value of the criterion parameter we used was typically $10^{-3}W^2m^{-3}$ which ensured a rapid and reliable convergence. This procedure is thus used to plot the intensity profile for different incoming intensities.

For the simulation, the device is divided into a number of layers to allow for the accurate calculation of the saturation behaviour which is important in terms of determining the dynamic range. Typically, the size of each layer in the TPA region is taken to be around 15 nm ($<\lambda_0/10n$ at 900 nm).

For optical pulses which are long compared with the cavity lifetimes (typically very high finesse semiconductor microcavity lifetimes are in the order of a few ps), the optical field standing wave regime (steady state) is attained, so the photocurrent laser pulse response of the cavity can be taken to be the same as in the CW case.

Expression for the k wavevector :

We now focus on the k propagation constant and thus the TPA intensity dependant refractive index change contributions. The first contribution comes from the non-linear refractive index n_2. A good review of non- linear refractive index and TPA is given in ref [26]. From this analysis, it is possible to see that when working close to the bandgap (where the β coefficient is the highest), the non-linear refractive index n_2 is dramatically increased, so the device dynamics can be drastically reduced. This effect has recently been observed in bulk AlGaAs semiconductor microcavities [42]. In theory, for degenerate TPA, there is one wavelength where n_2 is null. At this wavelength, positive and negative contributions from the TPA coefficient β in the Kramers-Kronig relations cancel out each other. From this study [26], the $n_2=0$ wavelength is located around $h\nu/E_g=0.7$. In practise, the real n_2 will be of the order of

10^{-17} m^2/W, and we will show in the following that this contribution has little impact on the device dynamics.

The second contribution comes from the generation of carriers. This effect has been shown to be a predominant one in self-phase modulation [43], and could possibly be the reason why a long delay transmission change is seen after a short pulse in recent experiments on GaN [13]. The TPA photogenerated carriers induce refractive index changes via band-filling and the plasma effect. The refractive index change per carrier density pair, far from the band edge in the bandgap, can be approximated by [41]:

$$\sigma_n = -\frac{q^2}{2\omega^2 \varepsilon_0 n_0 m_{eff}} \frac{E_g^2}{E_g^2 - (\hbar\omega)^2} \qquad (12)$$

where m_{eff} is the reduced effective mass of the electron-hole pair, n_0 the linear refractive index and E_g the bandgap energy.

As an example, for AlGaAs with $E_g = 1.77eV$, $\lambda = 0.9\mu m$, $m_{eff} = 0.07m_0$, $n_o = 3.48$, we get $\sigma_n = -4.2\ 10^{-27} m^3$.

In the pulsed regime, if the pulse duration τ_p is much shorter than the carrier lifetime but less than the cavity lifetime, then the number of photogenerated carriers is:

$$N = \frac{\beta I_0^2 \tau_p}{2\hbar\omega} \sqrt{\frac{\pi}{2}} \qquad (13)$$

for a pulse defined by :

$$I(t) = I_0 e^{-t^2/\tau_p^2} \qquad (14)$$

As our model is a steady state one, we cannot take the temporal carrier index change into account. To overcome this problem without losing accuracy of the description, we have taken an average carrier density seen by the pulse, i.e. *N/2*.

Finally, the k wavevector in the transfer matrix method is simply replaced by :

$$k = \frac{2\pi n}{\lambda} - i\frac{\beta I}{2} - i\frac{\alpha}{2} \qquad (15)$$

where :

$$n = n_0 + n_2 I + \sigma_n \frac{N}{2} \qquad (16)$$

As an example, using (12), with $|n_2|=1.\ 10^{-17}$ m^2/W [36], $|\sigma_n|=4.2\ 10^{-27} m^3$, $\tau_p=10ps$ and a carrier density $N=10^{19} cm^{-3}$, we get $n_2 I=4.10^{-4}$ while $|\sigma_n|N/2=2.10^{-2}$. This carrier induced refractive index change contribution is thus much greater than the nonlinear refractive index change $n_2 I$.

The photocurrent is calculated by integrating the absorbed intensity inside the depleted region of the photodiode:

$$I_{PC} = \int_0^L \frac{\eta_{TPA}\beta I^2(z)}{2E} + \frac{\eta_{SPA}\alpha I(z)}{E} dz \qquad (17)$$

Here E is the incident photon energy given in eV, and the η factors account for the TPA and SPA photocurrent conversion efficiency respectively. These factors have been estimated at 11% and 3% respectively in a recent publication [39] for a GaAlAs waveguide. These rather low values have been explained by recombination processes but no rigourous calculation of the optical mode injection, confinement factors and losses have been made. Instead, we assume a photocurrent conversion efficiency of 100% for both TPA and SPA in the undoped region and 0% in the n and p doped regions.

5. Device design for operation at 900nm

Various considerations must be taken into account when designing a cavity. The most efficient design will depend on the pump characteristics i.e. wavelength, duration, pump intensity. This results in a trade off between the speed, sensitivity and the dynamic range of the device.

First, as a Fabry-Pérot cavity response depends on the wavelength, the pulse spectral broadening $\Delta\lambda$ should be narrower than the spectral cavity resonance. The lower limit for a transform-limited pulse duration is given by $\Delta\lambda(\text{nm})=1.18/\tau_p(\text{ps})$ at λ=900nm. In the following, we will consider a pulse with a 10ps duration, thus having a minimal spectral width of 0.23nm. The cavity must then have a FWHM resonance wider than 0.23nm. This limits the mirror reflectivities and hence the enhancement factor achievable.

We have chosen AlGaAs/GaAs material with an active layer with a bandgap of around 700 nm, since it is possible to grow high reflectivity Distributed Bragg Reflectors (DBR) quite easily. The other question to assess is whether to use quantum wells as the active material. Using a vertical cavity and a normal incident beam, only the TE mode is used, so no exciton resonance appears in the TPA spectrum [37]. Even if the Coulomb/exciton enhancement factor is high above the bandgap, the use of quantum wells can cause carrier retrapping and hence reduce the device time response, due to reduction of carrier mobility along the growth axis [42]. Moreover, the use of quantum wells requires a very high quality growth, since any defect at the Quantum Well (QW)/barrier interface could increase the SPA absorption [39]. Reverse voltage application has been shown to improve device response, since photogenerated carrier can be swept out of depletion region rapidly, but care must be taken to avoid the enhancement of linear absorption via the Franz-Keldysh / Quantum Confined Stark Effects. Shallow quantum wells or thin barriers could thus be a good compromise for speed [40] and β optimisation due to the Coulomb/exciton effect.

Recently, Metal Semicondutor Metal (MSM) photodetectors using low temperature growth GaAs, have shown very fast TPA response <500 fs [12] at 1.5µm, but unfortunately, the introduction of defects also increases linear absorption [44,45] which drastically increases the optical intensity threshold where TPA becomes predominant over SPA photocurrent. We estimated the lower limit of the TPA dynamics for this device to be around 500 GW/m^2, which is a factor of ~100 higher than what could be expected by a defect free material with a residual linear absorption of 0.1cm^{-1}.

Following all these remarks, for a TPA response at 900nm, we simulated a AlGaAs/GaAs cavity using an active bulk material with a bandgap near 700nm (i.e. $Al_xGa_{1-x}As$ with x ~ 0.25). This bandgap ensures that the Franz-Keldysh absorption is kept below 0.1cm^{-1}, which can be taken as a lower intrinsic absorption value of the material by impurities or defects.

6. Simulation Results

We now present the results for two microcavity devices (A and B) and a non-cavity device (C). A and B consist of two $Al_{0.5}Ga_{0.5}As$/AlAs λ/4n Bragg mirrors (Fig. 3). The back Bragg mirror has 35.5 pairs (~99.86%) for both simulated devices while the front Bragg contains 5.5 pairs (R_1=66%) for device A, and 15.5 pairs (R_1=93.7%) for device B. Device C is Anti-Reflection (AR) coated on both facets and the active region is a λ/n $Al_{0.25}Ga_{0.75}As$ bulk semiconductor for all the devices. The cavity lifetime τ_{cav} of device A was calculated to be 0.6ps.

In the simulation, we also took into account the linear and non-linear absorption and refractive index of the mirrors.

Following [26], the parameters used are:

β_{Bragg}=0.008cm/MW, α_{Bragg}=20cm^{-1} , n_2=1.10^{-17}m^2/W, σ= -2.10^{-27}m^{-3} , β_{act}=0.02cm/MW, α_{act}=0.1cm^{-1}, λ=900nm, and the average power and current (upper and right scales) have been calculated with Ω=10μm, τ_p=10ps f=80MHz.

We have described the optical pulse incident on the cavity by:

$$I(r,t) = I_0 e^{-r^2/\Omega^2} e^{-t^2/\tau_p^2} \qquad (17)$$

and the peak intensity is then:

$$I_0 = \frac{W}{f\Omega^2 \pi^{3/2} \tau_p} \qquad (18)$$

where *W* is the average laser power and *f* is the laser repetition rate (Hz).

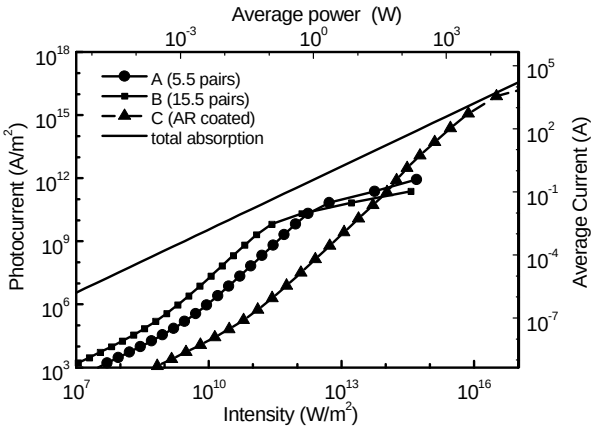

Fig. 3. Photocurrent (average current) versus intensity (average power), for the two simulated cavity devices and a non- cavity device.

As expected, a dramatic improvement on intensity is seen when inserting the active material into a FP cavity. Here an enhancement factor F is ~ 235 is reached with the device B over the 'non-cavity' device C. This in excellent agreement with the simple model explained in section

4, which also gives a factor of 235 enhancement (In fact, this simple model is exactly the same as the TMM as soon as we can take the empty resonator assumption). The equivalent TPA length of device C is then 5.4mm ($3\times235^2/8\times\lambda/n$). Moreover, as the FWHM of this cavity is ~ 1nm, no drop of the response due to pulse spectral broadening is expected for pulses down to 10ps duration (τ_{cav} ~ 1.6ps).

However, as mentioned earlier, the dynamic range of the FP microcavity device is much lower by a factor of 1000: the upper limit of the dynamic range in that case is not due to the total absorption, but to the generated carrier refractive index change in the structure which shifts the resonance wavelength of the device. Reverse voltage application could somewhat help to reduce the refractive index change by reducing the lifetime of the carriers inside the cavity (to a few ps).

We have recently applied this model successfully to a AlGaAs semiconductor microcavity [46].

7. Summary

In conclusion, we have theoretically studied the TPA effect in semiconductor microcavities for high speed all-optical sampling and demultiplexing applications in OTDM systems. Since TPA depends on the square power of the intensity, a high TPA photocurrent enhancement factor is expected using a Fabry-Perot microcavity (factor of a few thousands). We have also investigated the dynamic range of such a device and showed the requirements of device design in terms of speed, wavelength and pulse duration. By designing a semiconductor microcavity optimised for use as a TPA detector in either autocorrelation or demultiplexing applications, it

should be possible to develop highly sensitive and high-speed components for use in high speed optical communication systems. Furthermore, this example and model are however general enough to be implemented to other similar TPA devices, such as Resonant Cavity Schottky [47] or MSM [48] photodetectors which could reduce the carrier stacking in the Bragg mirrors and hence increase the device speed.

Acknowledgements

This work is supported by Enterprise Ireland, Glasnevin, Dublin 9, Ireland under grant No. SC/00/245.

References:

1. Y. Takagi, T. Kobayashi, K. Yoshihara, S. Imamura, "Multiple and single shot autocorrelator based on two photon conductivity in semiconductors," Optics Lett. 17, 658-660 (1992).
2. F.R. Laughton, J.H. Marsh, A.H. Kean, "Very sensitive two photon absorption GaAs/GaAlAs waveguide detector for an autocorrelator," Electronics Lett. 28, 1663-1665 (1992).
3. F.R. Laughton, J.H. Marsh, D.A. Barrow and E.L. Portnoi, "The two-photon absorption semiconductor waveguide autocorrelator," IEEE J. Quantum Electron. 30, 838-845 (1994).
4. H.K.Tsang, L.Y.Chan, J.B.D.Soole, H.P.LeBlanc, R.Bhat and M.A.Koza, "High sensitivity autocorrelation using two-phototn absorption in GaInAsP waveguides," Electron. Lett. 31, 1773-1775 (1995).

5. Z. Zheng, A. M. Weiner, J.H. Marsh and M. M. Karkhanehchi, "Ultrafast Optical Thresholding based on Two-Photon Absorption GaAs Waveguide Photodetectors," IEEE Photon. Technol. Lett. 9, 493-495 (1997).
6. J. K. Ranka, A. L. Gaeta, A. Baltuska, M. S. Pschenichnikov, and D. A. Wiersma, "Autocorrelation measurement of 6-fs pulses based on the two-photon-inducedphotocurrent in a GaAsP photodiode," Optics Lett. 22, 1344-1346 (1997).
7. T. Feurer, A. Glass, and R. Sauerbrey, "Two-photon photoconductivity in SiC photodiodes and its application to autocorrelation measurements of femtosecond optical pulses," Applied. Physics B. 65, 295-297 (1997).
8. D. T. Reid, M. Padgett, C. McGowan, W. E. Sleat, and W. Sibbett, "Light emitting diodes as measurement devices for femtosecond laser pulses," Optics Lett. 22, 233-235 (1997).
9. D. T. Reid, W. Sibbett, J. M. Dudley, L. P. Barry, B. Thomsen, and J. D. Harvey, "Commercial semiconductor devices for two photon absorption autocorrelationof ultrashort light pulses," Appl. Opt. 37, 8142-8144 (1998).
10. J. U. Kang, J. B. Khurgin, C. C. Yang, H. H. Lin, G. I. Stegeman, "Two-photon transitions between bound-to-continuum states in AlGaAs/GaAs multiple quantum well," Appl. Phys. Lett. 73, 3638-3640 (1998).
11. L. P. Barry, B. Thomsen, J. M. Dudley, and J. D. Harvey, "Autocorrelation and ultrafast optical thresholding at 1.5 mm using a commercial InGaAsP 1.3 mm laser diode," Electronics Lett. 34, 358-359 (1998).
12. H. Erlig, S. Wang, T. Azfar, A. Udupa, H.R. Fetterman, and D. C. Streit, "LTGaAs detector with 451fs response at 1.55µm via two-photon absorption," Electron. Lett. 35, 173-174 (1999).
13. C.-K. Sun, J.-C. Liang, J.-C. Wang, F.-J. Kao, S. Keller, M. P. Mack, U. Mishra, and S. P. Denbaars, "Two-photon absorption study of GaN", Appl. Phys. Lett. 76, 439-441 (2000).

14. M. Dabbicco and M. Brambilla, " Dispersion of the two-photon absorption coefficient in ZnSe," Solid State Commun. 114, 515-519 (2000).
15. J. Manning and R. Olshansky, "The carrier-induced index change in AlGaAs and 1.3μm InGaAsP diode Lasers," IEEE J. Quantum Electron. 19, 1525-1530 (1983).
16. H.K. Tsang, P.P. Vasilev, I.H. White, R.V. Penty, and J.S. Aitchison,, "First demonstration of two-photon absorption in a semiconductor waveguide pumped by a diode laser," Electron. Lett. 29, 1660-1661 (1993).
17. K. Ogawa and M. D. Pelusi, "High -sensitivity pulse spectrogram measurement using two-photon absorption in a semiconductor at 1.5μm wavelength," Optics Express 7, 135-140 (2000).
18. J. M. Dudley, L. P. Barry, J. D. Harvey, M. D. Thomson, B. C. Thomsen, P. G. Bollond, R, and R. Leonhardt, "Complete characterization of ultrashort pulse sources at 1550 nm," IEEE J. of Quantum Elect. 35, 441-450 (1999).
19. Jing Yong Ye, M. Ishikawa, Y. Yamane, N. Tsurumachi, and H. Nakatsuka, "Enhancement of two-photon excited fluorescence using one-dimensional photonic crystals," Appl. Phys. Lett. 75, 3605-3607 (1999).
20. C.C. Lee and Y. Fan, "Two-photon absorption with exciton effect for degenerate valence bands," Phys. Rev. B. 9, 3502-3516 (1974).
21. J. H. Bechtel and W. L. Smith, "Two-photon absorption in semiconductors with picosecond laser pulses," Phys. Rev .B. 13, 3515-3522 (1976).
22. A. Vaidyanathan, A.H. Guenther, and S.S. Mitra, "Two-photon absorption in several direct-gap crystals," Phys. Rev. B. 21, 743-748 (1980).
23. A. Vaidyanathan, A.H. Guenther, and S.S. Mitra, "Two-photon absorption in several direct-gap crystals- an addendum," Phys. Rev. B. 22, 6480-6483 (1980).
24. H. S. Brandi and C. B. De Araujo, "Multiphoton absorption coefficients in solids : a universal curve," Journ. Of . Physics C : Sol State Phy. 16, 5929-5936 (1983).

25. B. S. Wherrett, "Scaling rules for multiphoton interband absorption in semiconductors," J. Opt. Soc. America B 1, 67-72 (1983).
26. M. Sheik-Bahae, D. C. Hutchings, D.J. Hagan and E. Van Stryland, "Dispersion of bound electronic nonlinear refraction in solids," IEEE J. Quantum Electron. 27, 1296-1309 (1991).
27. A. R. Hassan, "Two-photon absorption in an indirect-gap semiconductor quantum well system. II: Excitonictransitions," Phys. Stat. Sol. B Basic Res. 186, 303-313 (1994).
28. M. Dabbicco and I. M Catalano, "Measurement of the anisotropy of the two-photon absorption coefficient in ZnSe near half the band gap," Opt. Commun. 178, 117-121 (2000).
29. M.H. Weiler, "Nonparabolicity and exciton effects in two-photon absorption in zincblende semiconductors," Solid State Comm. 39, 937-940 (1981).
30. A. Pasquarello and A. Quattropani, "Gauge-invariant two-photon absorption in quantum wells," Phys. Rev. B 38, 6206-6210 (1988).
31. A. Shimizu, "TPA in QW near bandgap ," Phys. Rev. B. 40, 1403-1406 (1989).
32. K. Tai, "Two-Photon absoprtion spectroscopy in GaAs quantum wells ," Phys. Rev. Lett. 62, 1784-1787 (1989).
33. A.Shimizu, T.Ogawa, and H.Sakaki, "Two-photon absorption spectra of low-dimensional semiconductors," Surf. Sci. 263, 512-517 (1992).
34. A. Shimizu, T. Ogawa and H. Sakaki, "Two-photon absorption spectra of quasi low-dimensional systems," Phys. Rev. B.45, 11338-11341 (1992).
35. J. B. Khurgin and S. Li, "Two-photon absorption and nonresonant nonlinear index of refraction in the intersubband transitions in the quantum wells," Appl. Phys. Lett. 62, 126-128 (1993).
36. C. C. Yang, A. Villeneuve, G. I. Stegeman, C. H. Lin, and H. H. Lin, "Anisotropic two-photon transitions in GaAs/AlGaAs multiple quantum well waveguides," IEEE J. Quantum Electron. 29, 2934-2939 (1993).

37. A. Obeidat and J. Khurgin, "Excitonic enhancement of two-photon absorption in semiconductor quantum well structures," J. Opt. Soc. Am. B 12; 1222-1227 (1995).
38. M. N. Islam, C. E. Soccolich, R. E. Slusher, A. F. J. Levi,W. S. Hobson, and M. G. Young, "Nonlinear spectroscopy near half-bandgap in bulk and quantum well GaAs/GaAlAs waveguides," J. Appl. Phys. 71, 1927-1936 (1992).
39. P. M. W. Skovgaard, R J Mullane, D N Nikogosyan, and J G McInerney, "Two-photon conductivity in semiconductor waveguide autocorrelators," Optics Commun. 153, 78-82 (1998).
40. M. B. Yairi, C. W. Coldren, D. A. B. Miller and J.S. Harris., "High-speed optically controlled surface-normal optical switch based on conductive diffusion ," Appl. Phys. Lett. 75, 597-599 (1999).
41. A. T. Obeidat, W. H. Knox and J. B. Khurgin, "Effects of two-photon absorption in saturable Bragg reflectors used in femtosecond solid state lasers," Optics Express 68, 1 (1997).
42. S. Sanchez, C. De Matos, and M. Pugnet, "Instantaneous optical modulation in bulk GaAs semiconductor microcavities," Appl. Phys. Lett. 78, 3779-3781 (2001).
43. T. G. Ulmer, R. K. Tan, Zhou Zhiping, S. E. Ralph, R. P. Kenan, C. M. Verber, and A. J. Springthorpe, "Two-photon absorption-induced self-phase modulation in GaAs-AlGaAs waveguides for surface-emitted second-harmonic generation," Optics Lett. 24, 756-758 (1999).
44. W. Schade, J. Preusser, D. L. Osborn, Y. Y. Lee, J. deGouw, S. R. Leone, "Spatially Resolved femtosecond time correlation measurements on a GaAsP photodiode," Optics Commun. 162, 200-203 (1999).
45. Y.J. Chiu, S.Z. Zang, S.B. Fleischu, J.E. Bowers, and U.K. Mishra, "GaAs-based, 1.55 µm high speed, high saturation power, low-temperature grown GaAs p-i-n photodetector," Electron. Lett. 34, 1253-1254 (1998).
46. H. Folliot, M. Lynch, A. L. Bradley, L. A. Dunbar, J. Hegarty, J. F. Donegan, L. P. Barry, J. S. Roberts and G. Hill, "Two-photon absorption photocurrent enhancement in bulk AlGaAs

semiconductor microcavities," Appl. Phys . Lett. 80, 1328-1330 (2002).

47. D. S. Golubovic, P. S. Matavulj and J. B. Radunovic, "Resonant cavity-enhanced Schottky photodiode modelling and analysis," Semicond. Sci. Technol. 15, 950-956 (2000).
48. D. M. Gvozdic, P. L. Nikoloic and J. B. Radunovic, "Optimization of a resonant cavity enhanced MSM photodetector," Semicond. Sci. Technol. 15, 630-637 (2000).